5G Communication with a Heterogeneous, Agile Mobile network in the Pyeongchang Winter Olympic CompetitioN

Grant agreement n. 723247

Deliverable D3.6
mmWave backhauling & fronthauling implementation

Date of Delivery:	20 Apr 2018
Editor:	Marko Pettissalo (Nokia)
Associate Editors:	
Authors:	Gosan Noh (ETRI), Junhyeong Kim (ETRI), Heesang Chung (ETRI), Ilgyu Kim (ETRI), Harri Mustajärvi (Nokia), Marko Leinonen (UOULU)
Dissemination Level:	PU
Security:	Public
Status:	Final
Version:	V1.02
File Name:	5GCHAMPION_D3.6_Final.pdf
Work Package:	WP3

Title:	Deliverable D3.6: mmWave backhauling & fronthauling implementation	
Date: 20-04-2018		**Status: Final**
Security: Public		**Version: V1.02**

Abstract

This deliverable provides the results of the implementation of the key elements for backhauling developed in the 5GCHAMPION project. There will be two different demonstration systems, one for EU and one for Korea. From the stationary EU test bed point of view, the key topic here is the implementation of the Antenna Unit, HW Mechanics and SW and interface towards existing and proprietary demonstration provided by Nokia.

Korean high speed train testbed shows design and implementation of the baseband and radio units and those integration.

Index terms

5G, mmWave, backhaul link, implementation, antenna.

Contents

List of Acronyms

3GPP	3rd Generation Partnership Project
5G	5th Generation
5GTN	5G Test network
AGC	automatic gain control
BB	Baseband
BRU	Backhaul Radio Unit
CA	Carrier aggregation
CC	Component carrier
C-RAN	Cloud radio access network
CRC	Cyclic redundancy check
dBi	decibel isotropic
DU	Digital unit
EIRP	Effective isotropic radiated power
EU	European union
GaN	Gallium nitride
GP	Guard period
HW	Hardware
IF	intermediate frequency
KPI	Key performance indicator
KR	Korea
LNA	low noise amplifier
LO	local oscillator
LoS	line-of-sight
MCS	Modulation coding scheme
MHN-E	Mobile Hotspot Network Enhancement
MIMO	Multiple-input-multiple-output
MME	Mobility Management Entity
MMIC	monolithic microwave integrated circuit
mmW	millimeter wave
MUX	Multiplexer
MWB	Mobile wireless backhaul
OFDM	Orthogonal frequency-division multiplexing
OIP	output intercept point
PA	Power amplifier
PCB	Printed circuit board
PoC	Proof of Concept
QAM	Quadrature amplitude modulation
QPSK	Quadrature Phase Shift Keying
RF-DFE	Radio Frequency Digital Frontend
RoF	Radio-over-Fiber
RSSI	Received signal strength indicator
RU	Radio unit
SDN	Software defined networking
SFBC	Spatial frequency block code
SNR	Signal-to-Noise Ratio
SPDT	Single point double throw
TBS	Transport block size

TDD	Time Division Duplex
TE	Terminal equipment
UE	User equipment
WP	Work package

Table of Figures

1 Introduction

EU mmW backhaul test bed i.e. demonstration platform is introduced at the high level and we describe implementation of Antenna Unit and it's SW. Implementation of integration of demonstration platform and Antenna Units is discussed. Additional details of the internal implementation of the Antenna Unit can be found in 5GCHAMPION D3.3 [1]. Measurement results can be found from 5GCHAMPION D6.4 [2]

Regarding the mmWave-based backhaul transceiver for high speed train, we describe the design and implementation of baseband and RF front-end. In addition, some test results are provided.

2 Key components of the EU mmWave transceiver platform

In this chapter, implementation of the key components for the EU mmWave backhaul transceiver platform are introduced. The developed mmWave Antenna Unit HW and Mechanical implementation from 5GCHAMPION WP3 Task 3.1. will be introduced firstly, followed by implemented Antenna Unit SW. Third portion of this chapter will be high level description of the existing mmWave demonstration platform offered by Nokia.

3 Overview of the demonstration platform

The demonstration platform provides features and KPIs as listed in the previous deliverables D2.1 [3] and D2.2 [4]:

In the Figure 1, 5G BRU comprises of three physical units; BBU, TRX Radio Unit and Antenna Unit. Two complete set of these systems are used for the mmW backhaul demonstration, pointing directly to each other as the typical wireless backhaul link application.

5G BRU provides point-to-point access between fixed locations and thus mobility, scheduling etc higher level protocol functionalities are not needed. 5G BRU assembles IP Packets to BB L1 blocks to be transmitted using mmW Antenna Unit.

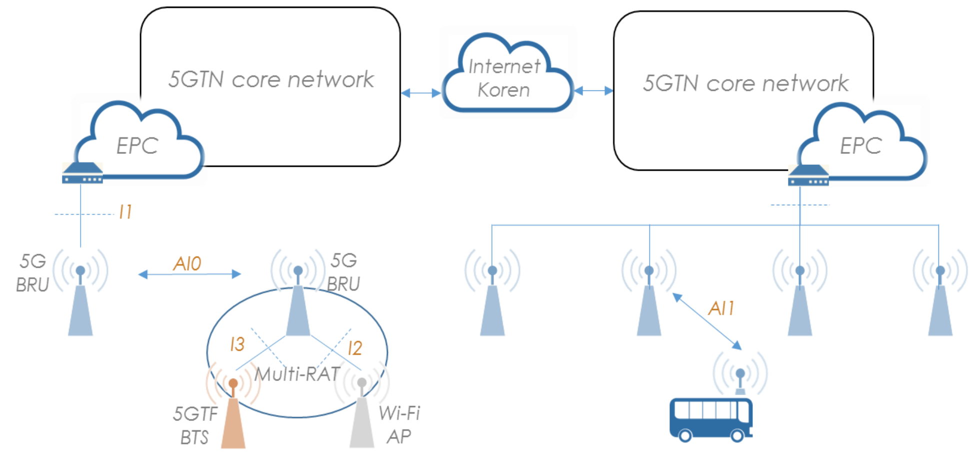

Figure 1 Illustration of 5GCHAMP

Figure 2 below show the key components, using green color to indicate the actual building blocks implemented in this project.

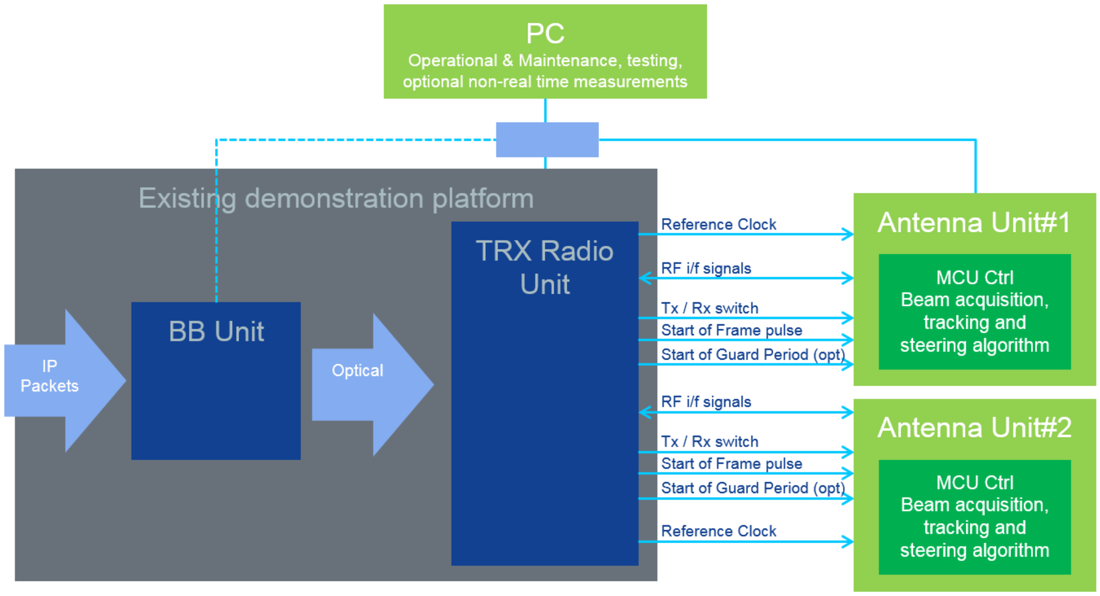

Figure 2 Functional split of different modules in the 5GCHAMPION EU mmW backhaul testbed

Figure 3 5GCHAMPION EU mmW Backhaul testbed

BBU unit is separated from TRX Radio Unit and Antenna Units and is connected to TRX Unit via optical cable, carrying IQ-samples over CPRI. System includes two Antenna Units. In **Erreur ! Source du renvoi introuvable.** and , the platform illustration and functional block illustrations are provided, respectively.

The BB unit implements a LTE x5 type BB and numerology:

MIMO-OFDM
with 100MHz Carrier Component
up-to 64QAM modulation.
Multiple Carrier Components can be aggregated in the frequency domain, reaching an overall maximum bandwidth of 800 MHz

Operational frequency at 26.5-29.3 GHz, focus on 26.5 to 27.5 GHz used in the Olympics.

Table 1 Design goals for EU mmW backhaul testbed

Design Parameters	Values
Frequency	28 GHz
Bandwidth	up-to 800MHz
EIRP	up-to 60dBm
Modulation order	QPSK, 16QAM, 64QAM
Antenna configurations	2x2 MIMO
Maximum throughput of MWB (demonstration)	up-to 2.5Gbps

3.1 The Antenna Unit:

The implemented Antenna Unit is composed of:

- An auxiliary board (AUX) with an MCU. The MCU provides control functionalities of the RF components including, phase-shifters, RF-input attenuator, power amplifiers, carrier frequency oscillator, RSS measurements and input/output connectivity with external boards Phase-shift control,
- Two RF boards for dual polarization transmissions with RF beamforming capabilities
- Two planar phased array with 8x2 antennas built as 2x2 subarray
- Mechanics

3.1.1 Implementation of Antenna Unit mechanics

Device main enclosure consist of milled aluminum frame and polymer based antenna cover. These main parts establish core mechanics with gaskets and PWB covers. Core mechanics function is to provide needed cooling capacity, grounding, and protection for PWB’s. Antenna cover material and thickness is optimized taking account material availability.

Main Properties:

- Dimensions: (WxHxD) 410 x 655 x 80mm
- Environmental protection: IP 42

Additional parts (Outer enclosure, Fan frame, fan assembly, top/bottom caps, mounting bracket) will provide follow functions:

- Establish final outlook of antenna module
- Enables Forced cooling
- Provide needed grip for handling & installation

- Enables installation with tilting option.

Module top level layout

- RF and Control PWB's are separate and each have dedicated EMI covers, Figure 5.
- All external interfaces are located to bottom surface of unit, Figure 4 and 5.
- All interconnections inside antenna module are done via cables.

Figure 4 Developed Antenna Unit Mechanics

3.1.2 Thermal Solution

Forced cooling is selected as it enables greatly smaller unit size than fanless, especially when cooling is single sided (antenna on the other side)

- All electronics are thermally coupled to main heat sink
- Thermal vias are used for components on opposite side of the board than heat sink

Three 60x60x25 mm fans are used to pull air through the unit

- A visual cover is forming a duct around the fins and preventing air by passing the fins

- Fans are PWM controllable to keep unit in more constant temperature and reducing acoustics noise

3.1.3 Implementation electronics and antenna array of antenna unit

The antenna unit includes two similar radio (RF) boards, one AUX board and two antenna array modules. The system design of the radio solution of the antenna unit is described in detail in [6]. The same reference includes information of the component selection, as well. The antenna module is described in detail in [7]. There are two versions of the antenna array modules with are -45° and +45° polarizations. The antenna modules are removable and those can be attached to both antenna module locations.

The block diagram of the antenna unit is shown below

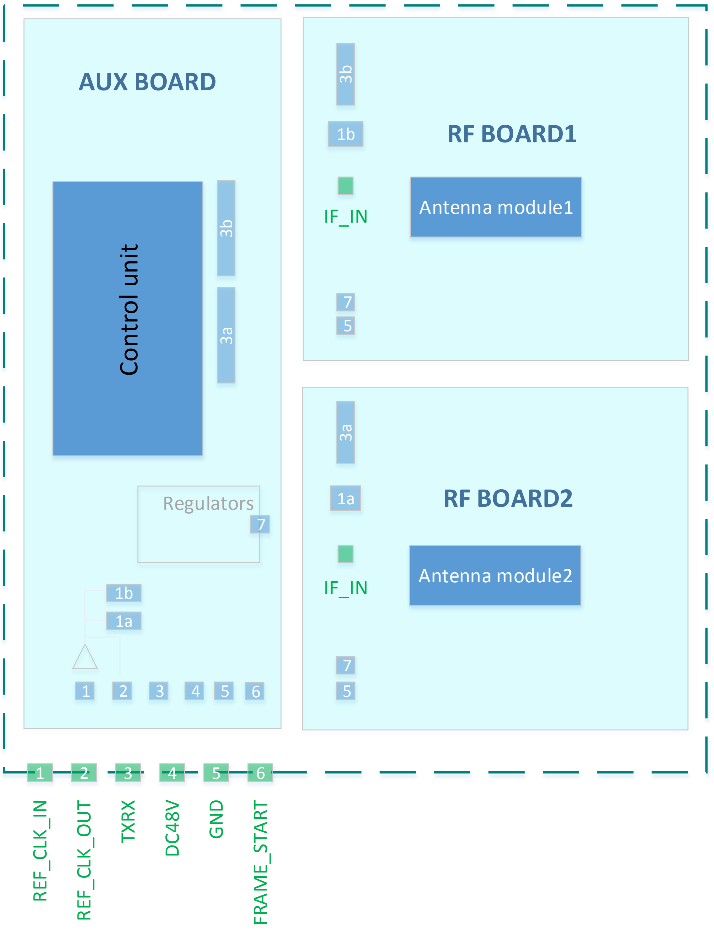

Figure 5 Block diagram of the EU mmW antenna unit

The RF boards are connected to the TRX unit with an analog interface. The radio board includes up- and down-conversions of IF signal from/to the final mmW operation frequency. There are 16 signal paths in the RF board and 16 physical antenna connectors.

The photographs of the RF board and AUX boards are shown in figures 6 and 7, respectively [6]. The photograph of the antenna array board is shown in figure 8 [6].

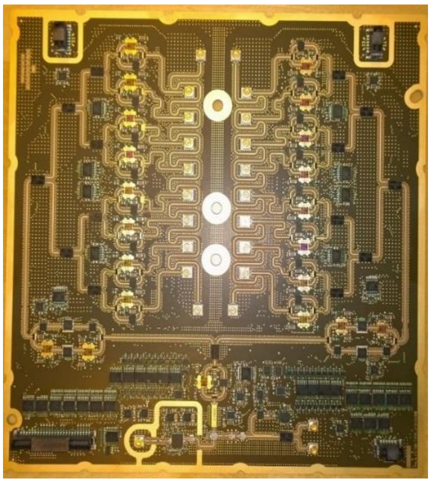

Figure 6. Photograph of RF board prototype

The AUX-board which generates operational voltages of the radio unit, distributes control and clock signals. Additionally, the processor board is attached to the AUX-board with a header connector.

The AUX board generates the operational voltages of the antenna unit, which are marked as in the table 2. The +48V is coming into the antenna unit and it is marked as DC48V in the block diagram and in the interface signal table below. The AUX board includes voltage regulators for +20V, +6V and -15V operational voltages. These voltages are fed to the RF board with wide connection wires. The +20V is used for operational voltage of power amplifiers. The +6V and sub-voltages of this are used for other RF components on the RF board. The -15V and sub-voltages of this are used to bias the PAs and RF switches. The +6V is supplied to the MCU control board which is the blue coloured printed wire board (PWB) top of the AUX board in the photograph below.

The control unit (MCU) is the STM32 Nucleo-144 development board with STM32F429ZI microcontroller in LQFP144 package. It controls the operation of the antenna unit (beamformer, local oscillator, power measurement, scheduling and amplifiers). The control unit is synchronized with the TRX radio unit via timing signals that indicates TX/RX slot as well as radio-frame start (10ms periodic signal). In operational mode, the control unit can autonomously change the received and transmitted signal power by controlling the radio boards, adapt beam direction and beam width based on some optimization criteria, e.g., maximize the signal-to-noise-ratio. Also in the set-up with four antennas, two control units are networked and configured in a master-slave mode.

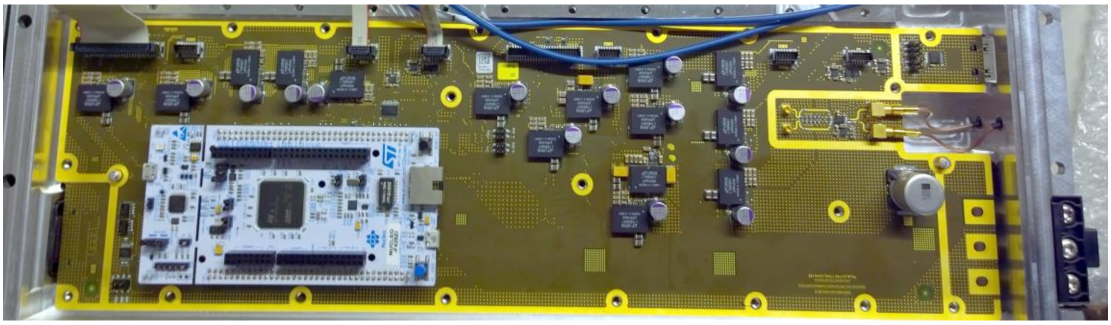

Figure 7. Photograph of the AUX board with MCU attached top of it

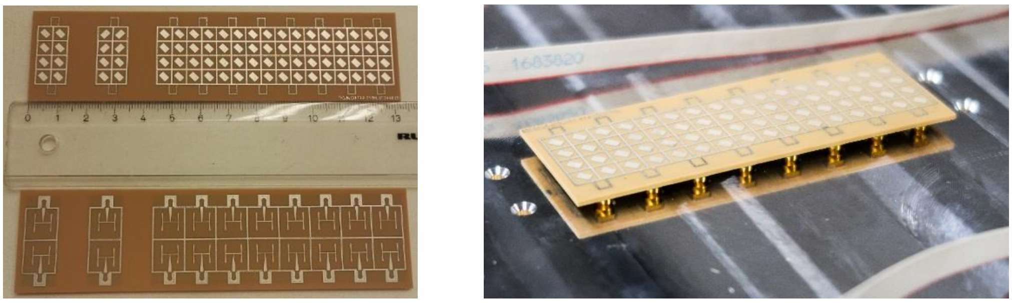

Figure 8 Photograph of the prototype antenna array..(Left) Antenna array with testing subarray. (Right) Antenna mounted on the platform

Table 2 Interfaces of the antenna unit

Signal reference number	Signal name	Signal function
1	REF_CLK_IN	Reference clock input
1a and 1b	-	Filtered reference clock signal for RF signal generation
2	REF_CLK_OUT	Reference clock output
3	TXRX	Transmission and reception timing signal
3a and 3b	-	Control signals of the radio boards
4	DC48V	48V operational voltage
5	GND	Ground signal
6	FRAME_START	Start of the signal frame
7	-	Regulated operational voltages of the radio board
IF_IN	IF_IN	Communication signal interface

3.2 The TRX Radio Unit

The TRX Radio Unit includes following functionalities: Interface to BBU via optical able, Complex Numerically Controlled Oscillator (NCOs), Interpolation/decimation filter, RF impairment correction, ADC/DAC, Wideband IQ up/down, Synthesizer and LO.

The key functions enabling the integration are the Rx/Tx RF intermediate frequency signals and control and timing signals towards the developed Antenna Unit. These are discussed in more details in the Chapter 5.

In addition, there are fan and power supply modules for the TRX Radio Unit. All Units can be seen in the Figure 3 5GCHAMPION EU mmW Backhaul testbed

3.3 The BB Unit, Baseband Unit

Figure 9 show the logical architecture of BBU. It consists of several sub-modules including encoder and decoder, downlink modulator, and uplink demodulator. Additionally, the BBU includes the front-end for pre-coding and FFT in addition to cell searcher. BBU interfaces to the corresponding L1 controller. Additionally, the BBU also provides I/Q samples and timing control signaling for the TRX Unit and for both Antenna Units.

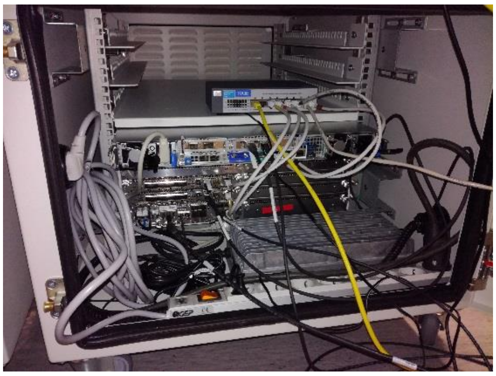

Figure 9 BB Unit assembled in the rack

4 Implementation of RF control software

Figure 10 SW Architecture of the Antenna Unit

The RF-control software is running in the MCU which is located in the antenna unit which is described in chapter 3.1.3

The RF-control software architecture is depicted above [6]. It comprises of:

- **Application layer**: BTS and UE software. These applications manages the overall functionality of the radio board. In the 5GCHAMPION project they are mostly responsible of the beam alignment procedure and beamforming.
- **Middleware**: The middleware comprises of all control threads, which will run simultaneously, communicate via message passing interface (MPI) and use the hardware abstraction layer (HAL) library.
- **Hardware abstraction layer**: The HAL is a library of functionalities that control the drivers.
- **Driver**: The drivers are HW specific and include procedures that operate directly on signals (input/output of the MCU).

4.1 Thread Model

The middleware contains control threads mentioned below:

Middleware Thread name	Thread ID value
SCHEDULER_CTRL	0
BF_CTRL	1
PA_CTRL	2
FREQUENCY_CTRL	3
AGC_CTRL	4
COM_TX_CTRL	5
COM_RX_CTRL	6
RSS_CTRL	7

Each thread follows the following implementation model. All threads are initiated simultaneously and become active at the occurrence of an event.

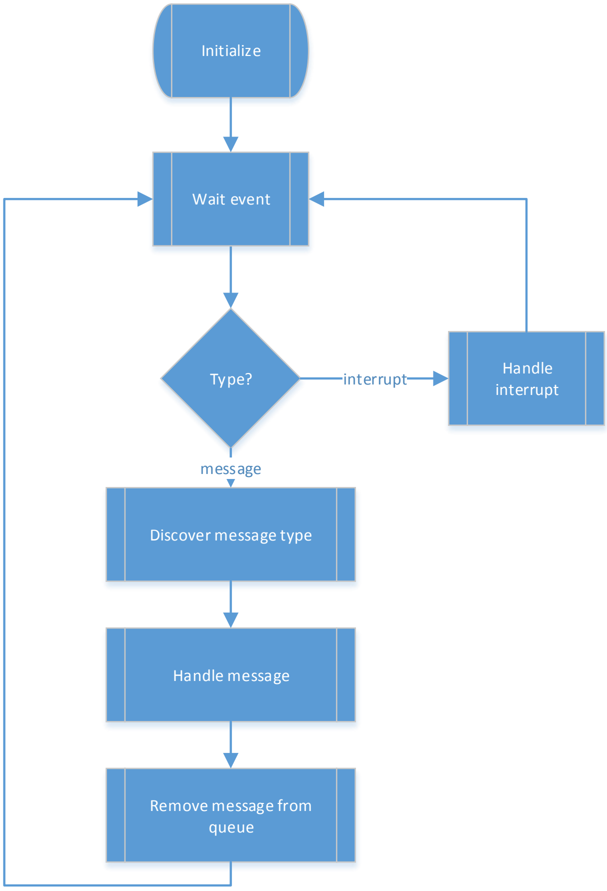

Figure 11: Thread model

Events are notified by signals that, in some cases, are also associated to a message. The message has a source, a destination and a payload. Middleware

The middleware logic for the software comprises of the following control threads:

4.1.1 Beamformer_ctrl_thread

Purpose

The thread acts as a middleware between the input received via MPI from communication_ctrl_thread and beamforming algorithm functionality. Beamformer control thread decodes the MPI message and calls the corresponding lower level functions.

Features

The thread includes functionalities such as setting the beamforming type and options resetting the all beamforming related options to initial values, tuning the beamforming based on individual phase shifter values, setting the triggering mode. Each one of these functionalities are performed with the lower level of the architecture using MPI communication protocol.

4.1.2 Communication_ctrl_thread

Purpose

The thread acts as a bridge and helps in communicating the data between Nucleo and external application layer using Ethernet packets and message passing mechanisms. In its implementation, the data received from application layer, are decoded based on their PDU id and sent to the corresponding control thread. Similarly, the thread receives information from other control threads via MPI and transmits the data to application layer via UDP.

Features

The thread includes functionalities such as ‘communication send’ and ‘communication receive’. ‘Communication send’ handles MPI thread communication where the message received from other control threads are to be transmitted via UDP to the application layer. ’Communication send’ handles RSSI and PA control thread transmissions to the application layer. Similarly, ‘communication receive’ helps in receiving the Ethernet packets from application layer and pass the information to RSS and PA control threads through MPI.

4.1.3 Frequency_ctrl_thread

Purpose

The thread acts as a controller of the local oscillator in the radio boards. It can be enquired from internal or internal applications.

Features

The thread contains functionalities such as set LO frequency, change LO frequency, reset LO frequency, switching on the synthesizer and switching off the synthesizer. Each one of these functionalities are performed with the lower level of the architecture using MPI communication protocol.

4.1.4 PA_ctrl_thread

Purpose

The thread helps in controlling the PA’s on RF boards. All the PA related information, coming from the application layer are received as MPI packets by this thread. Based on the received information, the logic then invokes corresponding HAL layer functionality related to PA’s.

Features

The thread includes functionalities such as adding a calibration value to PA, stop calibration of PA, Loading EEPROM at application layer with calibrated PA’s and enabling particular PA/LNA during calibration and debug phases. Each one of these functionalities are performed using MPI communication protocol.

4.1.5 RSS_ctrl_thread

Purpose

The thread reads RSSI signal information from HAL layer on the Nucleo and sends the information as MPI data to communication control thread.

Features

The thread includes functionalities such as reading a RSS signal from RF unit periodically, a single RSS read from RF unit and stop reading RSS signal periodically. Each one of these functionalities are performed using MPI communication protocol.

4.1.6 Scheduler_ctrl_thread

Purpose

This thread helps in scheduling the signal synchronization tasks, periodic RF beam alignments of the transceiver and handling communication between BTS and UE in application layer while fixing RF beam directions

Features

The thread maintains the synchronization between control threads by scheduling interrupts at the falling edge of transmission signal

4.1.7 Fan_ctrl_thread

Purpose

This thread controls the fan speed of the RF board.

Features

Based on temperature readings from the RF board internal sensors, temperature is kept within the optimal value range.

4.1.8 AGC_ctrl_thread

Purpose

This thread performs the automatic gain control on the receiving signal. It is key for handling mobility

Features

It operates on the beamformer attenuators to maintain the receiving signal power within the optimal operational range.

4.1.9 Hardware Abstraction Layer (HAL) and drivers

HAL library for this project consists of the abstraction of for example controlling local oscillator, power amplifier etc. More details can be found from 5GCHAMPION D3.3 [6].

5 Implementation of the TRX and Antenna Unit Control Interfaces

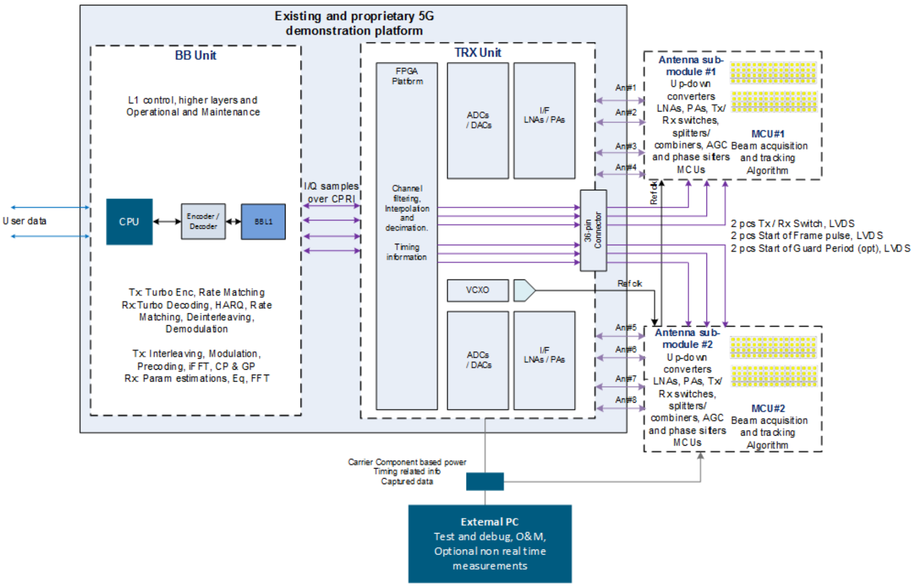

Figure 12 TRX Radio Unit and Antenna Unit interface signals

5.1 RF i/f and Reference clock

Table 3 RF Interface signal between TRX Radio Unit and Antenna Unit

	Design Parameters	Values
RF i/f	Frequency	few GHz
RF i/f	Bandwidth	400 / 800 MHz
Ref Clk	Frequency	230MHz

5.2 Digital Control signals

Digital control signals from the TRX Radio Unit related to beamforming and control timing are:

- Tx / Rx switch, indicating if there the ongoing OFDM symbol is meant to be Tx or Rx

- A pulse indicating start of the 10ms air frame
- Optional guard period indicator i.e. giving a pulse when guard period between OFDM symbols starts.

These signals are routed to both Antenna Units as differential digital signals. Also, some level of timing adjustment for each signal could be expected for fine tuning of the mmW backhaul demonstration system and integration. Signal are routed directly from existing 5G demonstration platforms TRX Unit.

Table 4 Digital Interface signals between TRX Radio Unit and Antenna Units

TRX Unit Connector	Design Parameters	Values
Green pair	Tx/Rx switch	LVDS
Red pair	Start of Air Frame	LVDS
Blue pair	Start of Guard Period	LVDS

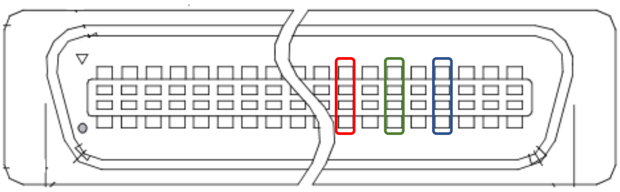

Figure 13 TRX Unit Connector for the implemented control signals.

5.3 Port for Captured IQ Data etc

In the TRX Radio Unit, there is allocated internal memory for capturing I/Q samples, that is possible to download via Operational and Maintenance Port. It's usability for the 5GCHAMPION project is under planning.

6 mmWave-based mobile backhaul transceiver design and implementation for high speed train

6.1 Baseband modem design

The mmWave-based backhaul transceiver of the MHN-E system is designed to provide a broadband mobile wireless backhaul (MWB) for high-speed trains running at speeds of up to

500km/h. The system architecture of the MHN-E system basically originate in the hierarchical two-hop network, which, as illustrated in Figure 14, consists of MWB links outside using millimeter-wave and onboard access links. Since this network concept has several well-known advantages [8], it has already been applied to many commercialized railway communication systems [9], and is also being considered as one of the potential deployment scenarios by both 3GPP and IEEE 802 [10].

In the MHN-E network, MHN digital unit (mDU) and MHN radio unit (mRU) are separated from each other and interconnected via optical fiber, which forms an efficient cloud radio access network (C-RAN). Each individual mRU with its corresponding mDU functions as a base station, hence has a unique cell ID different from others. As illustrated in Figure 14, the mRUs are deployed along the trackside, and two mRUs installed in the same location transmit sharp beams pointing to opposite directions. As a result, MHN terminal equipment (mTEs) mounted on top of both head and rear sides of the train could receive independent signals sent from mRUs of different sites simultaneously. Each mTE behaves like a single user connected to onboard access link providing mobile Internet service to user equipment (UEs) carried by passengers in the train.

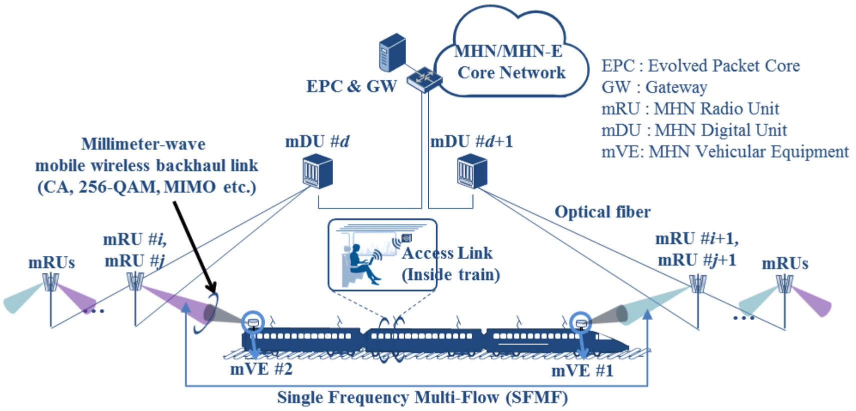

Figure 14 System architecture of MHN-E.

6.1.1 Frame structure

Considering that data traffic in high-speed scenarios is largely asymmetric in nature, where downloads typically accounts for most of the traffic, the DL is prioritized rather than UL in this case. In this regard, we focus on TDD for MHN-E. Like other cellular systems, as shown in Figure 15, TDD of MHN-E is able to offer configurable resource allocation between the downlink and uplink where time durations are changed as required. Figure 15 shows the TDD frame structure of the system. A subframe has 8 slots and each slot is 250-us long. Each slot contains 40 OFDM symbols. One symbol is 6.25-us long which is the sum of the reciprocal of a subcarrier spacing of 180 kHz (5.56 us) and a cyclic prefix length of 0.69 us. The second slot in each subframe of 2*ms*, l-th slot (l=1,9,17,25,33), is a special slot, which consists of downlink pilot time slot (DwPTS), guard period (GP), and uplink pilot time slot (UpPTS). Figure 15 also shows three different UL-DL configuration supported in MHN-E, and their corresponding ratios of DL to UL.

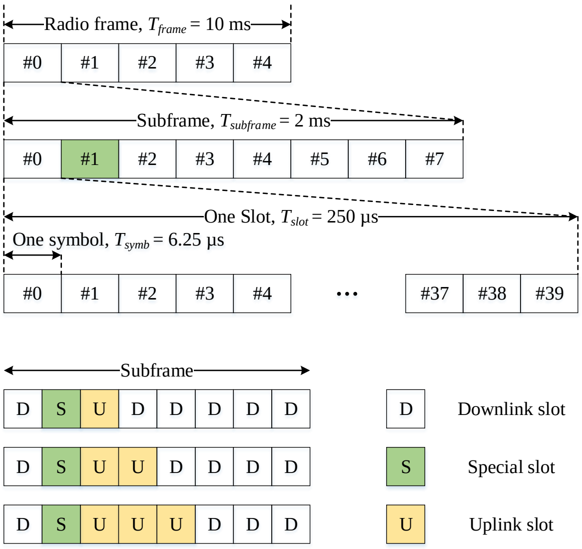

Figure 15 Frame structure of MHN-E system

Table 5 shows the details of numerology for the MHN-E system.

Table 5 Numerology for MHN-E system

Parameters	**Values**
Subcarrier spacing	180 kHz
Sampling clock rate (MHz)	184.32
OFDM symbol duration, no CP (us)	5.56
CP duration (us)	0.69
CP overhead (%)	12.4
Number of symbols per TTI	40
TTI duration (ms)	0.25
Frame duration (ms)	10
Number of RBs in frequency domain	50
Number of subcarriers per RB	12
FFT size	1024

6.1.2 Carrier aggregation

One of the main features included in the MHN-E specification is a frame structure enabling carrier aggregation (CA), efficient neighbor cell search and high-performance handover as shown in Figure 16. Each aggregated carrier, generally referred to as a component carrier (CC), has a bandwidth of 125MHz, and orthogonal frequency division multiplexing (OFDM) parameters of which are basically identical to that of the MHN-E [9]. The MHN-E allows the aggregation of a maximum of eight CCs to attain a total transmission bandwidth of up to 1GHz. Additionally, it is required that at least two CCs should be supported as mandatory and the different number of CCs, 2~8, can be configured depending on mTE capability. Each configured CC in the MHN-E system employs OFDM for both uplink (UL) and downlink (DL) transmissions.

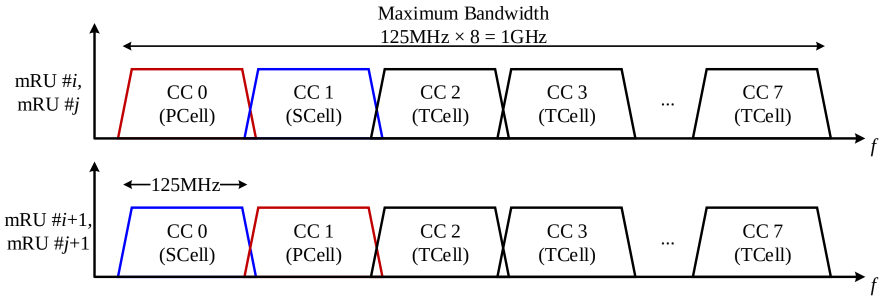

Figure 16 Contiguous intra-band carrier aggregation

In order to enable robust handover procedure in a HST environment, three different cell types are defined in the CA structure, which are primary cell (PCell), secondary cell (SCell), and tertiary cell (TCell) as shown in Figure 17. Each CC can be configured by one of the cell types. The first and second CCs are configured by either PCell or SCell depending on the location of mRU and the remaining CCs are configured by TCell.

As illustrated in Figure 17, the PCell is not only responsible for sending data and control channels, but also for sending MHN synchronization signal and cell information through MHN broadcast channel (M-BCH). The SCell and TCell, on the other hand, only send data and control information. The main difference between the two is that the SCell vacates the resource location where MHN broadcast channel (M-BCH) or synchronization signal is transmitted in the PCell to detect target cell signal without interference from serving cell.

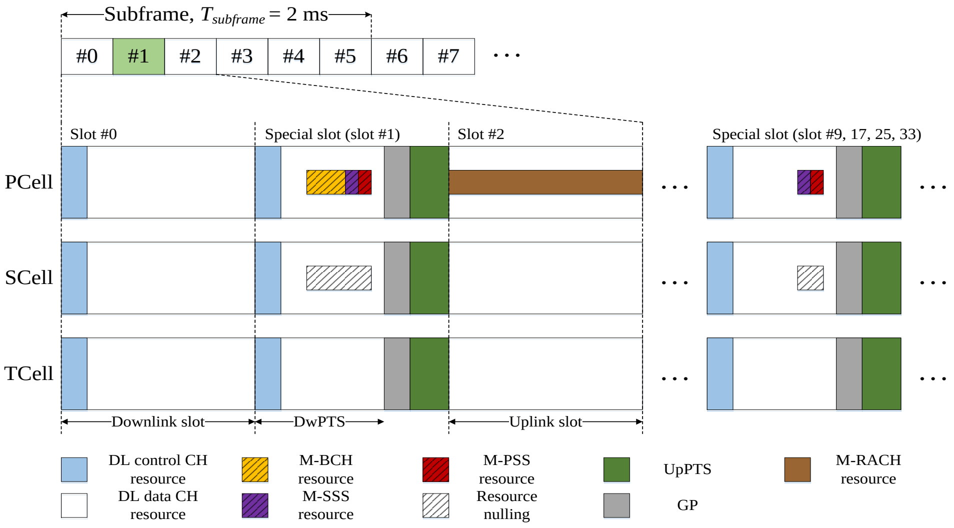

Figure 17 Frame structure enabling CA, efficient neighbor cell search and fast handover.

Additionally, MHN random access channel (M-RACH), mainly used to get access to the network and obtain timing alignment information to synchronize uplink transmissions, is designed to be transmitted only in the PCell. Since in most cases, there is no train/mTE or only one train/mTE in a cell, there is almost little possibility of collision among the requests coming from multiple mTEs. So, the design of M-RACH could be a contention-free-based, and its procedure can be significantly simplified as compared with that of Cellular systems.

6.1.3 Modulation and channel coding

This section describes modulation and channel coding schemes. Table 6 shows the table of modulation and coding schemes (MCSs) for downlink transmission.

Table 6 MCS table for downlink

MCS Index	modulation	coding rate x 1024	efficiency	Code Rate
0	2	120	0.2344	0.11718750
1	2	157	0.3057	0.15332031
2	2	193	0.3770	0.18847656
3	2	321	0.6270	0.31347656
4	2	449	0.8770	0.43847656
5	2	603	1.1768	0.58886719
6	4	301	1.1768	0.29394531
7	4	378	1.4766	0.36914063
8	4	434	1.6954	0.42382813
9	4	490	1.9141	0.47851563
10	4	553	2.1602	0.54003906
11	4	616	2.4063	0.60156250
12	4	658	2.5684	0.64257813
13	6	438	2.5684	0.42773438
14	6	466	2.7305	0.45507813
15	6	517	3.0264	0.50488281
16	6	567	3.3223	0.55371094
17	6	616	3.6123	0.60156250
18	6	666	3.9023	0.65039063
19	6	719	4.2129	0.70214844
20	6	772	4.5234	0.75390625
21	6	822	4.8193	0.80273438
22	6	873	5.1152	0.85253906
23	6	910	5.3350	0.88867188
24	8	683	5.3350	0.66699219
25	8	711	5.5547	0.69433594
26	8	797	6.2266	0.77832031
27	8	885	6.9141	0.86425781
28	Implicit TBS signaling with QPSK			
29	Implicit TBS signaling with 16QAM			
30	Implicit TBS signaling with 64QAM			
31	Implicit TBS signaling with 256QAM			

The usage of channel coding scheme and coding rate for TrCHs is defined in Table 7 and, the usage of channel coding scheme and coding rate for control information is summarized in Table 8. The code rate of Turbo coding applied to TrCH of both UL-SCH and DL-SCH is 1/3. A tail biting convolutional code with constraint length 7 and coding rate 1/3 is used for control information including DCI, MI, HI, UCI.

Table 7 Usage of channel coding scheme and coding rate for TrCHs

TrCH	Coding scheme	Coding rate
UL-SCH	Turbo coding	1/3
DL-SCH		

Table 8 Usage of channel coding scheme and coding rate for control information

Control Information	Coding scheme	Coding rate
DCI	Tail biting convolutional coding	1/3
MI	Tail biting convolutional coding	1/3
HI	Repetition code	1/6
UCI	Block code	variable
	Tail biting convolutional coding	1/3

6.1.4 Reference signal design

Figure 18 shows the mapping of downlink reference signals, which is cell-specific. The downlink reference signal is designed to use a lattice type allocation, and the allocation of the reference signals is for a total of two antenna ports. The period in the time domain is four symbols, and the period in the frequency domain is six subcarriers.

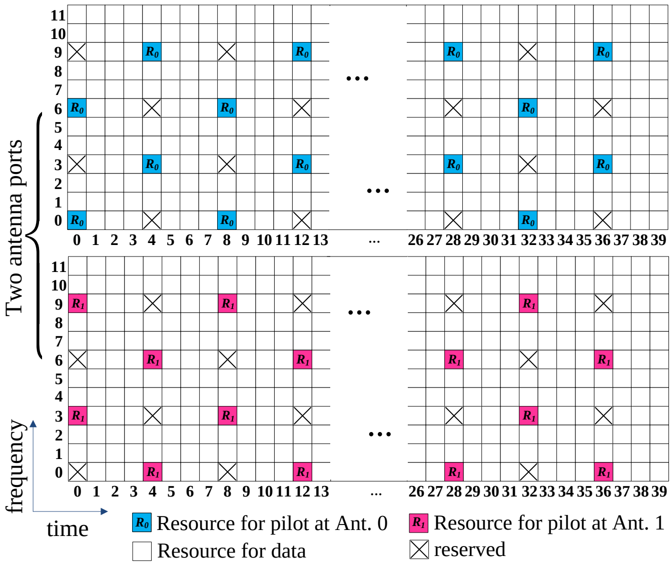

Figure 18 Mapping of downlink reference signal

Figure 19 shows the mapping of uplink reference signals, which is mTE-specific. The percentage of the symbols of the reference signals is 12.5%. In typical cellular systems like LTE, symbols for uplink reference signals are generally deployed in a regular interval. However, since in the uplink transmission, frequency offset caused by Doppler is twice larger than that of downlink, a new reference signal design is required. Therefore, the uplink reference signal in the MHN-E system is designed in a different way, where the first two reference signals in the time domain are arranged closer than the others in order to resolve the Doppler problem in a HST channel.

As shown in Figure 20, the frequency offset f_1 (blue line) that can be estimated by 2nd and 5th reference signals in time domain is ±26.67 kHz while the frequency offset f_2 (red line) that can be estimated by 5th, 14th, 23th and 32th reference signals in time domain pilots is ±8.89 kHz. The final frequency offset f_o can be calculated as follows:

$$f_o = \begin{cases} (f_1 + f_2)/2 & if\ |f_1| \le 8.89\,\text{kHz} \\ (f_1 + f_2)/2 + 8.89\text{kHz} & if\ f_1 > 8.89\,\text{kHz} \\ (f_1 + f_2)/2 - 8.89\text{kHz} & if\ f_1 < -8.89\,\text{kHz} \end{cases}$$

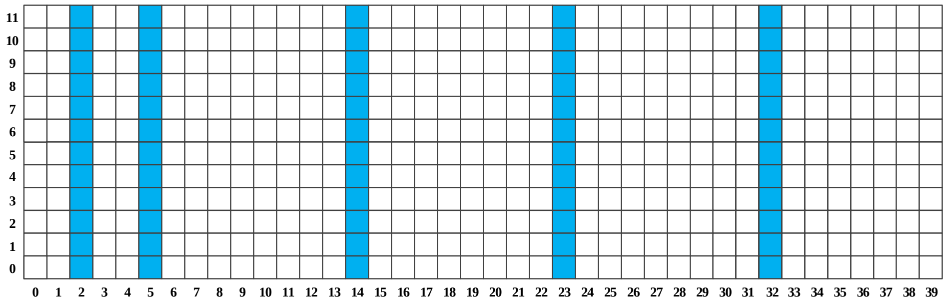

Figure 19 Mapping of uplink reference signal

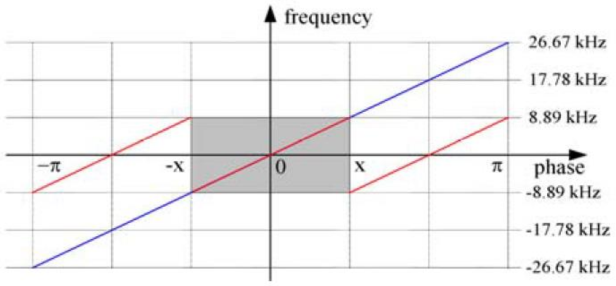

Figure 20 Uplink frequency estimation range

6.1.5 Doppler mitigation

The MHN-E system targets to support mobility up to 500 km/h. As seen in Figure 21, at that speed along with mmWave frequency bands, severe Doppler effect is expected, i.e., the maximum Doppler spread can be tens of kHz. In this case, the channel is highly time-varying and its estimation is not a trivial task. In order to well estimate such a high mobility channel, we allocate downlink reference signal such that the time interval between the two adjacent OFDM symbols containing reference signals is 25 us, which satisfies the Nyquist condition.

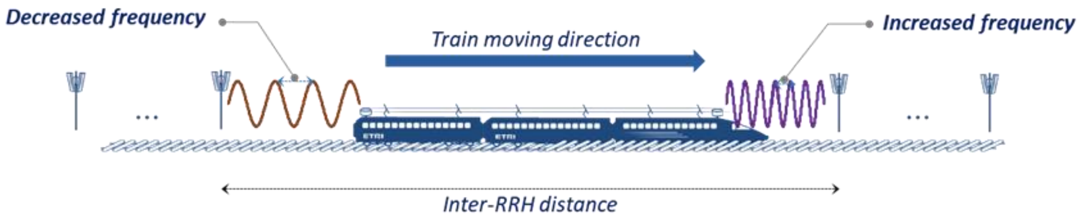

Figure 21 Doppler effect in HST

In addition to the Doppler spread, Doppler shift due to line-of-sight (LOS) components occurs large frequency offset, significantly degrading the link performance. The amount of Doppler shift is more significant for the uplink, i.e., doubled Doppler shift compared to the downlink due to the oscillator locked to the downlink signal. As discussed in the previous subsection, the uplink reference signal of the MHN-E system is designed to estimate the uplink frequency offset up to the range of [-26:67; 26:67] kHz. When the amount of frequency offset is correctly estimated, the Doppler-induced frequency offset can be efficiently compensated by, for example, automatic frequency control (AFC) in the time-domain.

6.1.6 Multi-antenna scheme

The channel characteristics of the HST scenario reveals strong LOS components thereby preventing rich scattering environments. Therefore, as seen in Figure 22, dual-polarized 2x2 MIMO scheme is employed, where vertically polarized and horizontally polarized components are independently transmitted. In a strong LOS channel, depolarization between the vertically polarized and horizontally polarized components are minimized. Although there will be some inter-polarization interference, these can be mitigated using receiver signal processing techniques.

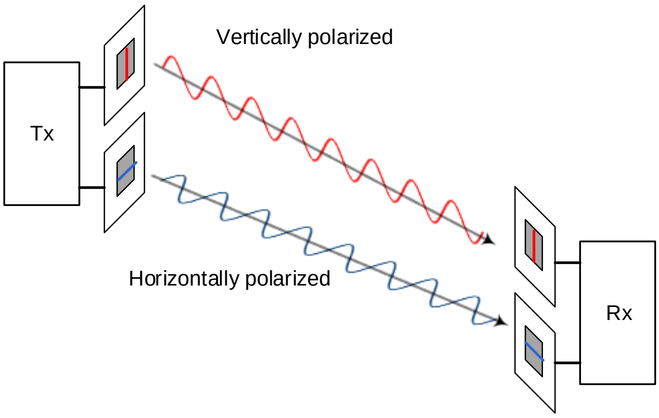

Figure 22 Polarized MIMO scheme

Considering high mobility, open-loop spatial multiplexing is employed. Although closed-loop spatial multiplexing better performs by selecting optimal codebook at the transmitter thanks to the channel state information feedback, the performance gain of the closed-loop spatial multiplexing is not guaranteed in the high Doppler scenario due to feedback delay.

6.1.7 Baseband platform design

General baseband modem designs are depicted in Figure 23 for mDU and in Figure 24 for mTE, respectively. Both mDU and mTE modems commonly contains transport channel (TrCH) encoder and decoder, modulator and demodulator, and front-end controller. Turbo coding/encoding and cyclic-buffer rate matching/recovery are implemented at the TrCH encoder and decoder. Front-end controller is responsible for controlling and monitoring the operation of the RF front-end. In the mTE modem, cell searcher is implemented, which acquires time and frequency synchronization, frame timing, and cell identity. For both mDU and mTE modems, interfaces to the corresponding L1 controller are configured.

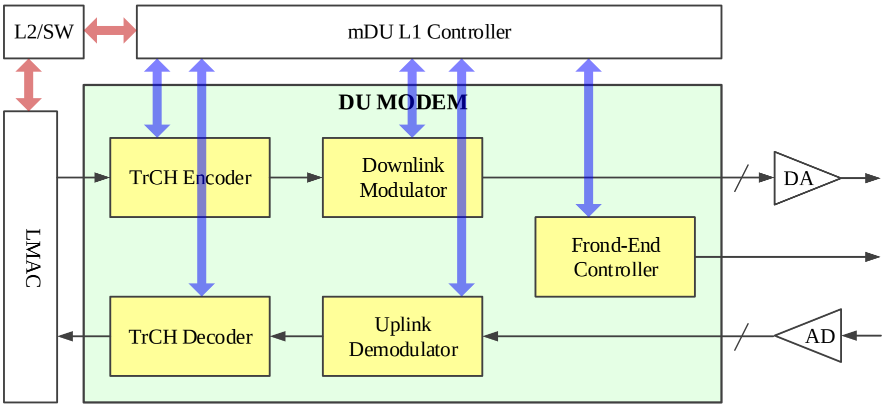

Figure 23 mDU baseband modem diagram

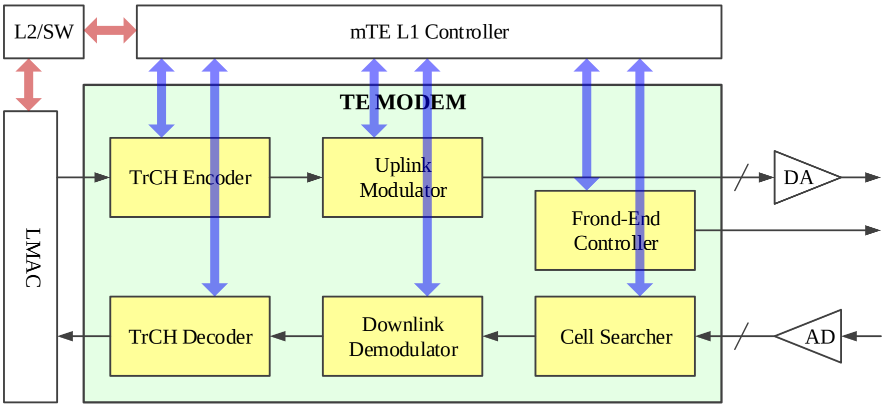

Figure 24 mTE baseband modem diagram

Requirements for the MHN-E baseband platform includes :

- Support for 5 Gbps data throughput
- Support for baseband modem functionalities
- Capability of L1 control
- Capability of transmission of MAC data/message from/to L2/L3 higher layers
- Support for diagnostic monitoring (DM)
- Support for RF interface

According to MHN-E specification, basic unit of transmission bandwidth or frequency assisnment (FA) for uplink and downilnk is 125 MHz. Simultaneous 8 FAs are supported. Baseband platform design for the MHN-E is shown in Figure 25. Using 5 FPGA, functionalities for the data transmission and reception of 8 FAs are processed. More specifically, 1 FPGA is used for the processing of the analog/digital interface, PCIe interface, and DDR memory interface. 4 FPGAs are used for the data processing, each of which is responsible for 2 FAs. Channel coded is processed using dedicated chip. DDR3 memory is employed to support the DM, which enables to read and write the I/Q data for the 8 FAs. PCIe Gen.2 IP is employed to process 5 Gbps data throughput.

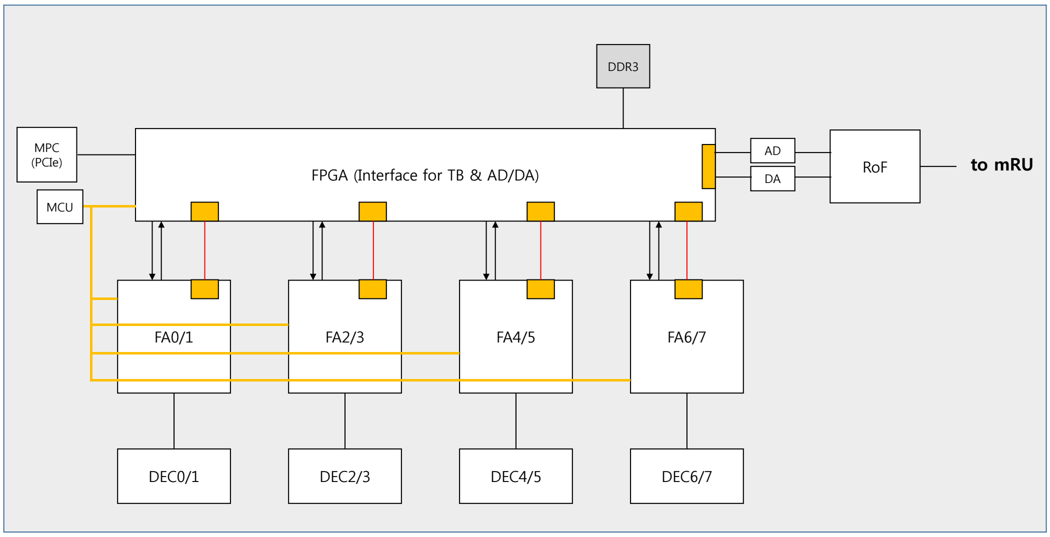

Figure 25 Baseband platform diagram

6.1.8 Baseband platform implementation

According to the above platform design, platform layout for implementation is provided, as seen in Figure 26. Main modem funtionalities such as modulation/demodulation modules are implemented using field-programmable gate array (FPGA) (Xilinx Kintex7 UltraScale XCKU115). Analog-to-digital (AD) and digital-to-analog (DA) converters operating with frequency of 1843.2 MHz is used. TI ADC32RF45 is used for AD converter which supports 4 Gsps. TI DAC38RF89 is used for DA converter which supports 8.4 Gsps. Micro controller unit (MCU) chip (STM32F746NGH6) is employed for L1 control. The PCIe interface is used between L2/L3 and mDU. The radio-over-fiber (RoF) is used to connect between mDU and mRU.

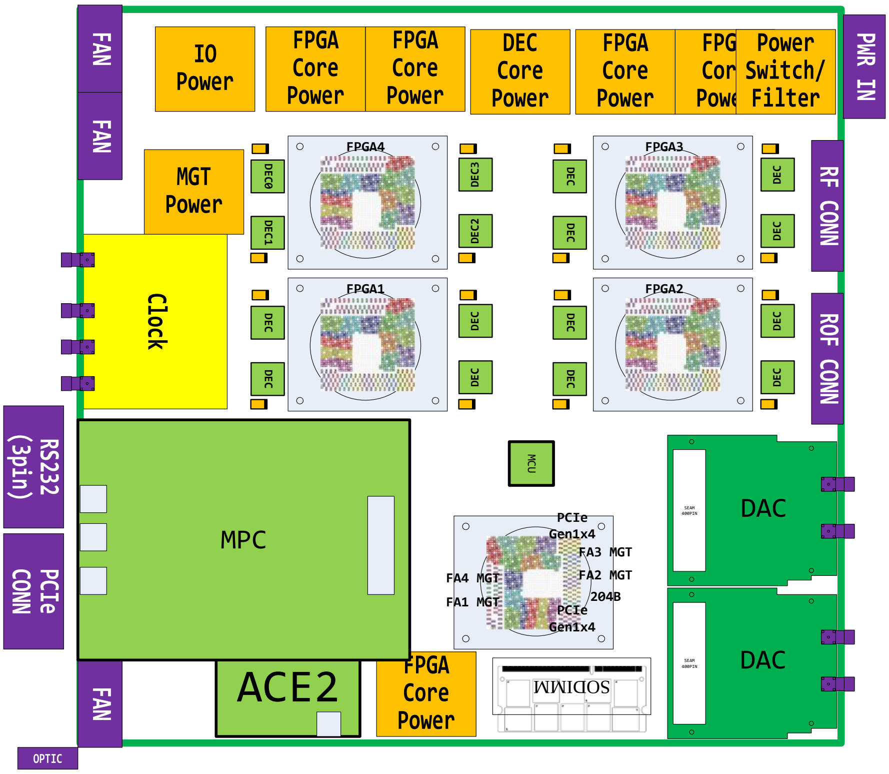

Figure 26 Baseband platform implementation layout

Figure 27 shows implemented mDU baseband modem board.

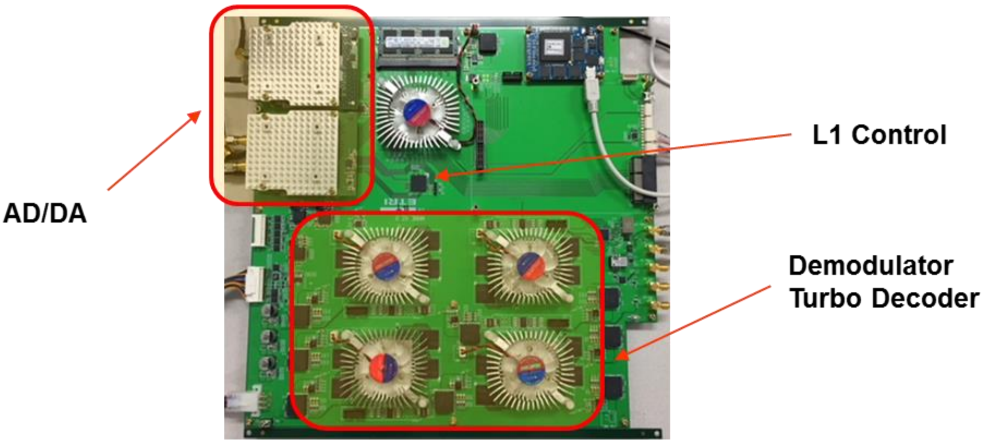

Figure 27 mDU baseband modem implementation

6.2 RF front-end design

6.2.1 RF design parameters

The RF design target is quite challenging: support for carrier aggregation of 8 component carriers (CCs) with the overall bandwidth of 1 GHz at the carrier frequency band of 25 GHz. The detailed RF design parameters are summarized in Table 9.

Table 9 RF design parameters

Common	Operating frequency	25.1432 ~ 26.1432GHz
	Band Width	1GHz
	DIF Frequency	1.3432 ~ 2.3432GHz
	TDD Switching Time	< 5usec
	TRX Isolation	≥ 55dB
TX	Output Power	> +17dBm(Avg)
	Gain	> 27dB
	Gain Flatness	± 3.0dB(TBD)
	TX Spurious	< -40dBc
	TX DIF Input	-15dBm(Total)
	TX EVM	< 4%(TBD)
RX	Noise Figure	< 8dB
	Input Level	-20dBm (Max.) ~ -57dBm (Min.)
	Gain	> 43dB
	Gain Flatness	± 3.0dB(TBD)
	Gain Control	≥ 0.5/31.5dB , ≥15dB
	DIF Output	-10dBm(Total)

6.2.2 RF design

The exterior and interior of mRU is depicted in Figure 28 and in Figure 29, respectively. There are 2 TX and 2 RX RF paths at the mRU. A power supply module, local oscillator module and radio-over-fiber (RoF) interface module are also included. RF assembly is done so as to satisfy the water protection IP65 and a certain vibration resistance level. mRU has an LED in its exterior which enables to display an alarm event. Debugging port for monitoring and controlling is also provided. Thermal analysis is carried out during the heat sink design and package size optimization.

Figure 28 mRU exterior

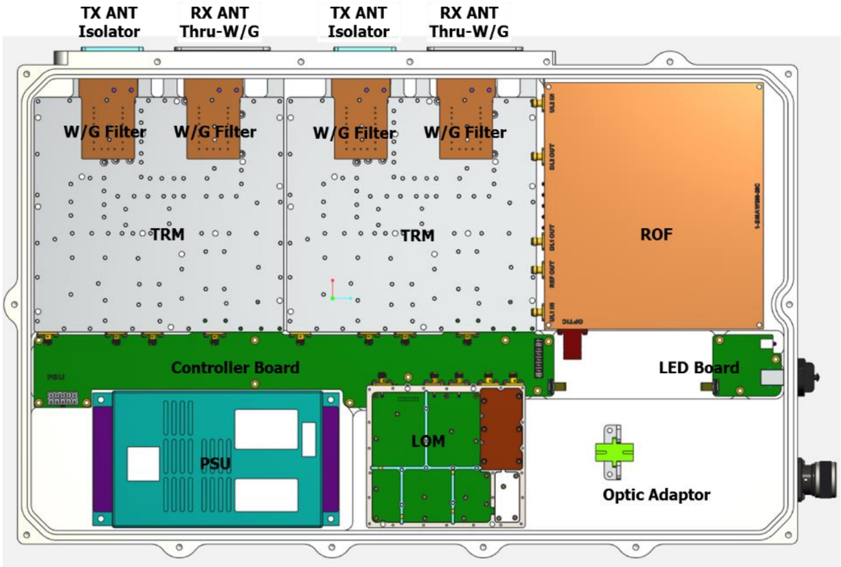

Figure 29 mRU interior

6.2.3 Antenna design

Slotted waveguide array antennas are employed in order to maximize the radiation efficiency with limited dimension as seen in Figure 30 for mRU and Figure 31 for mTE, respectively. Each TX antenna has 4x4 radiating elements with an array gain of 19 dBi. Each RX antenna has 6x6 radiating elements with an array gain of 22 dBi. The TX antenna should keep the regulatory output power in terms of equivalent isotropic radiated power (EIRP), i.e., the sum of the maximum output power and the array gain should be lower than 36 dBm. Dual-polarized transmission and reception is supported at the mRU TX and mTE RX, allowing 2x2 dual-polarized MIMO transmission in the downlink.

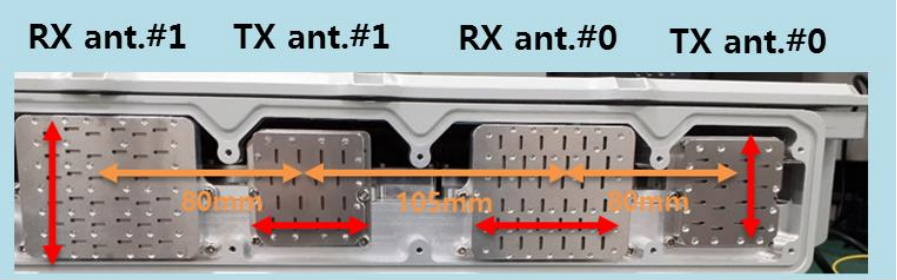

Figure 30 mRU antenna configuration

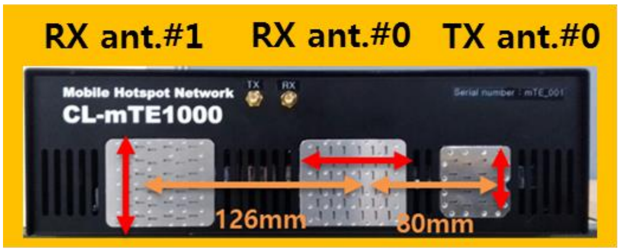

Figure 31 mTE antenna configuration

Beam patterns are depicted in Figure 32 for TX antenna (left) and RX antenna (right). The beam patterns are obtained via simulation. It can be seen that 3 dB beamwidth is 17.9-18.9 degrees for the TX antenna and 11.5-12.6 degree

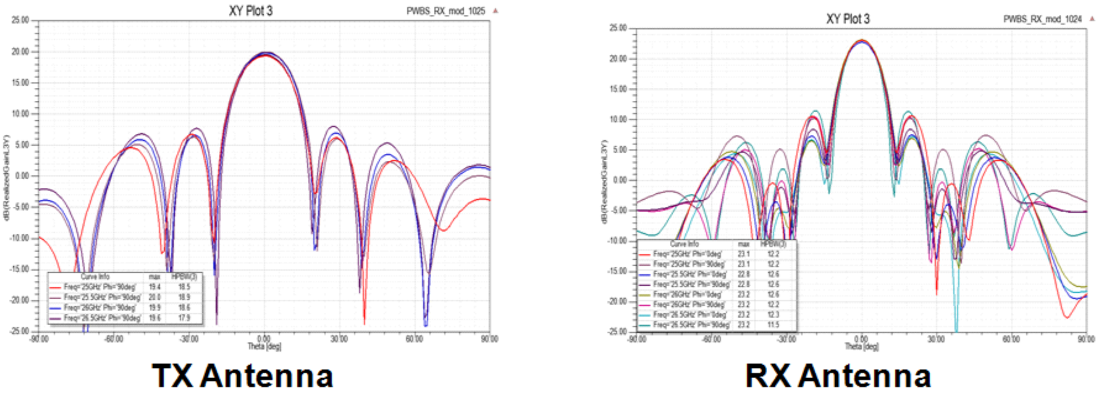

Figure 32 TX and RX antenna beam patterns

6.3 Testing procedures and preliminary results

6.3.1 Indoor lab test

Functionalities of the MHN-E system are tested under an indoor environment. A testbed configuration is shown in Figure 33. An mNB consist of an mDU (Digital Unit) and an mRU (Radio Unit). An mTE includes a baseband part and radio part in a module. The interface between higher layer and mDU modem is PCIe. The interface between mDU modem and mRU is RoF.

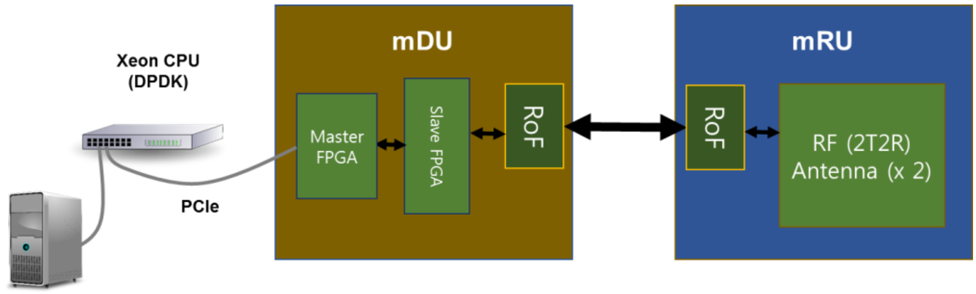

Figure 33 Testbed configuration

Higher layer protocol (L2/L3) stacks such as MAC, RLC, PDCP, RRC and NAS are implemented in software using on a Xeon processor. The L2/L3 implementation platform is shown in Figure 34.

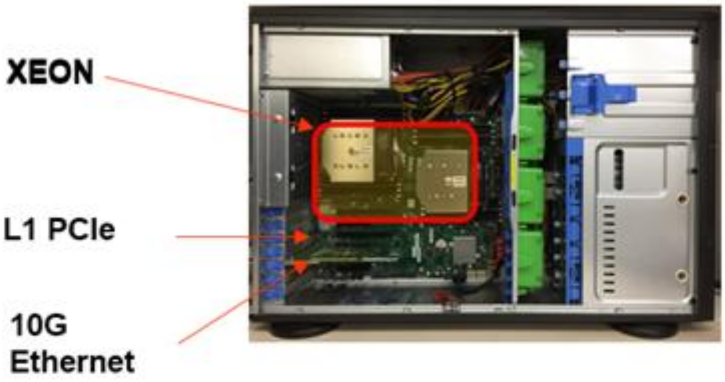

Figure 34 L2/L3 implementation platform

The actual testbed setup for indoor testing is shown in Figure 35. Figure 36 shows diagnostic monitors for the link, respectively. Employing a bandwidth of 1 Gbps and 2x2 polarized MIMO, the peak data rate of 5.2 Gbps is achieved.

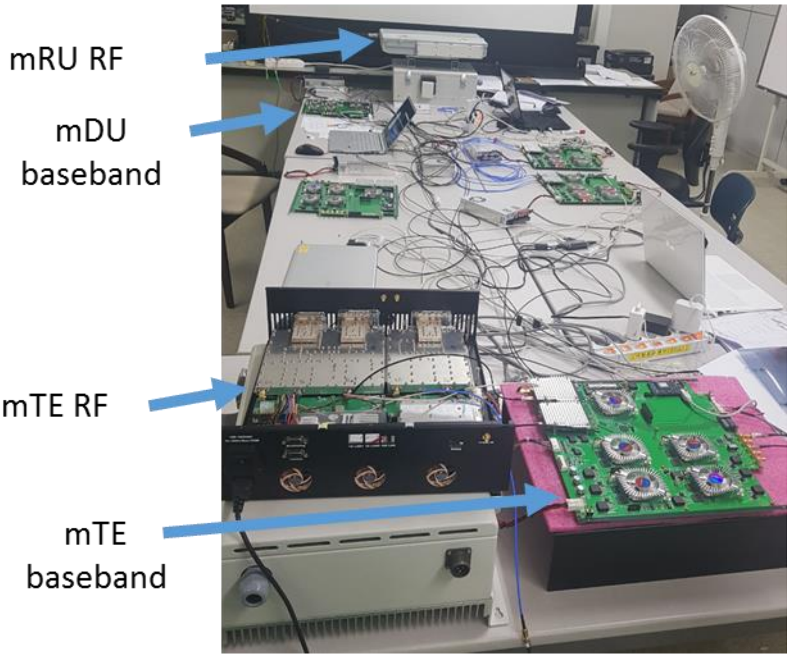

Figure 35 Test setup for indoor link

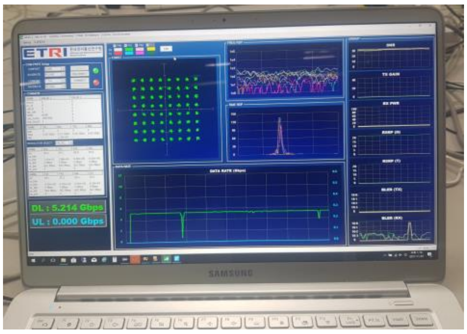

Figure 36 Peak data rates in diagnostic monitors

6.3.2 Subway field test

Real environments for the subway or high-speed trains are different from the indoor environment in many ways. First of all, the trains run under various channel environments such as the tunnels, rural, urban, viaduct, stations, mountains, etc. Therefore, it is meaningful to demonstrate the functionalities of the MHN-E system in the real world. The tunnel among many environments is very challenging since it represents strong and fast fading channel characteristics.

In this regard, the MHN-E system has been tested in the running subway trains of Seoul subway Line 8. Figure 37 shows a subway map of Seoul metropolitan area and a train path of Seoul subway Line 8 where the MHN-E systems was tested. There are three stations, Jamsil, Seokchon and Songpa from left to right in the figure. Four mRUs were installed between the Jamsil st. and Seokchon St. to cover the curved path. An mRU was installed near the Songpa

St. for the straight path. The locations of the five radio units were determined by a wave propagation test using mmWave-based MHN prototypes before this field trial.

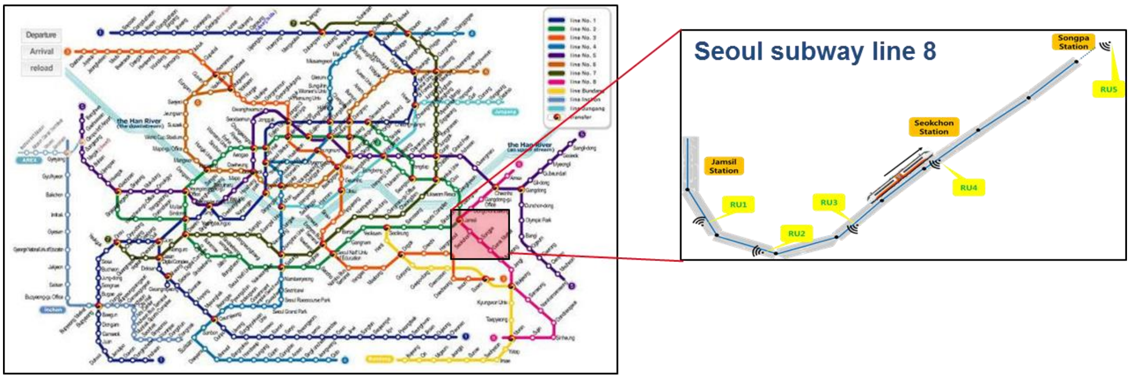

Figure 37 Seoul subway Line 8 path for a field trial

An mTE was installed in the engine room of the running train just behind the front window. If the mTE approaches the Jamsil St., it starts a random access to attach to the mNB. As the train runs through the route in the figure, the mTE receives and transmits signals from/to the mRUs on the nearest mRUs. When it passes the mRU, it carries out the handover procedure to connect to the next cell until it passes through the last mRU. Figure 38 illustrates a captured performance monitoring display that includes 64QAM constellation, frequency and time domain impulse responses and downlink and uplink data throughput. The green line (bottom) shows downlink data throughput. It keeps maintaining 1.25 Gbps of data rate most time. Four drop points indicate handover regions. In this field trial, the critical functionalities like handover and data throughput have been proven.

Figure 38 Measured performance of the MHN system in a field trial

7 Conclusion

In this report we have described implementation of key components of the 5GCHAMPION wireless backhaul solution, namely Antenna Unit HW, Mechanics and SW.

References

[1] 5GCHAMPION Deliverable D3.3 Beamforming antennas and front-end integration
[2] 5GCHAMPION Deliverable D6.4 System level testing of “proof of concept” phase 2
[3] 5GCHAMPION report “5GCHAMPION Architecture, API- and interface (D2.1),” 2017.
[4] 5GCHAMPION report “5GCHAMPION Key Performance Indicator and use cases (D2.2),” 2017.
[5] 5GCHAMPION report “5GCHAMPION Front-end design (D3.1)” 2017.
[6] 5GCHAMPION Deliverable “Beamforming antennas and front-end integration (D3.3),” 2017
[7] Sonkki M. et al, “Linearly Polarized 64-element Antenna Array for mm-Wave Mobile Backhaul Application,” EUCAP2018 conference, in press
[8] J. Kim and I. G. Kim, "Distributed antenna system-based millimeter-wave mobile broadband communication system for high speed trains," 2013 International Conference on ICT Convergence (ICTC), Jeju, 2013, pp. 218-222.
[9] S. W. Choi, H. Chung, J. Kim, J. Ahn, and I. Kim, "Mobile Hotspot Network System for High-Speed Railway Communications Using Millimeter Waves," ETRI Journal, vol. 38, no. 6, pp. 1042-1051, December 2016.
[10] 3GPP TR 38.913, “Study on Scenarios and Requirements for Next Generation Access Technologies,” 2016.